DOI 10.1007/s11141-022-10172-5
Radiophysics and Quantum Electronics, Vol. 64, No. 10, March, 2022
(Russian Original Vol. 64, No. 10, October, 2021)

PEDESTRIAN-INDUCED BRIDGE INSTABILITY: THE ROLE OF FREQUENCY RATIOS

I. V. Belykh,[1,2] **K. M. Daley,**[1] **and V. N. Belykh**[3,2] *

UDC 534

The emergence of the pedestrian-induced bridge instability is conventionally associated with crowd synchrony; however, this view has been challenged. In this paper, we use a bio-mechanical pedestrian model in the form of an active inverted pendulum to analyze the average contribution of a single pedestrian to possibly uncorrelated crowd dynamics and bridge oscillations. We obtained that depending on the ratio of the bridge vibration and walking frequencies, the pedestrian can amplify bridge vibration or, surprisingly, extract energy from the bridge and damp bridge oscillations. In particular, we show that different combinations of the bridge and pedestrian step frequencies corresponding to the same or close frequency ratios can trigger two drastically different bridge dynamics, with enhanced or suppressed oscillations far from the resonances.

1. INTRODUCTION

Christiaan Huygens, a Dutch mathematician, physicist, and astonomer, was the first to study the collective dynamics of mechanical oscillators [1]. In particular, he observed the emergence of anti-phase synchronization of two pendulum clocks, suspended on a wooden beam. Remarkably, the forces of the anti-phased clocks on the beam canceled each other out, thereby keeping the beam still [2–4]. Since Huygens's experiment, phase-locking and cooperative dynamics have been extensively studied in a wide spectrum of oscillator systems [5–10], including neural networks [11–13], lasers [14–16], and power-grids [17].

Pedestrian–bridge interactions are an important example of emergent complex dynamics in networks of mechanical oscillators. Many pedestrian bridges have experienced dramatic vibrations or even have collapsed due to the effects of dynamical pedestrian loading and/or mechanical resonance (see [18] for a detailed review of documented bridge instability cases).

The list of foot bridges that developed dangerous pedestrian-induced vibrations includes the Toda Park Bridge [19], Solférino Bridge in Paris [20], the London Millennium Bridge [21], the Maple Valley Great Suspension Bridge [22], the Singapore Airport's Changi Mezzanine Bridge [23], the Clifton Suspension Bridge [24], and the Pedro e Inês Footbridge [25].

The best-known example of the pedestrian-induced instability is the onset of large-amplitude lateral oscillations of the London Millennium Bridge, which occurred when the number of pedestrians exceeded a critical value [21,26]. That effect was originally attributed to synchronization of pedestrians' steps within the framework of Kuramoto model [27–29]. However, the role of crowd synchrony in triggering bridge wobbling was challenged later [18, 30, 31]. In particular, it was shown in [18] that the synchronization of pedestrians' steps is a consequence, not the cause, of the instability. In fact, even uncorrelated pedestrian motion can

* ibelykh@gsu.edu

[1] Department of Mathematics and Statistics, Georgia State University, USA; [2] Department of Control Theory, Lobachevsky State University of Nizhny Novgorod; [3] Department of Mathematics, Volga State University of Water Transport, Nizhny Novgorod, Russia . Translated from Izvestiya Vysshikh Uchebnykh Zavedenii, Radiofizika, Vol. 64, No. 10, pp. 777–786, October 2021. Russian DOI: 10.52452/00213462_2021_64_10_777 Original article submitted September 3, 2021; accepted October 28, 2021.

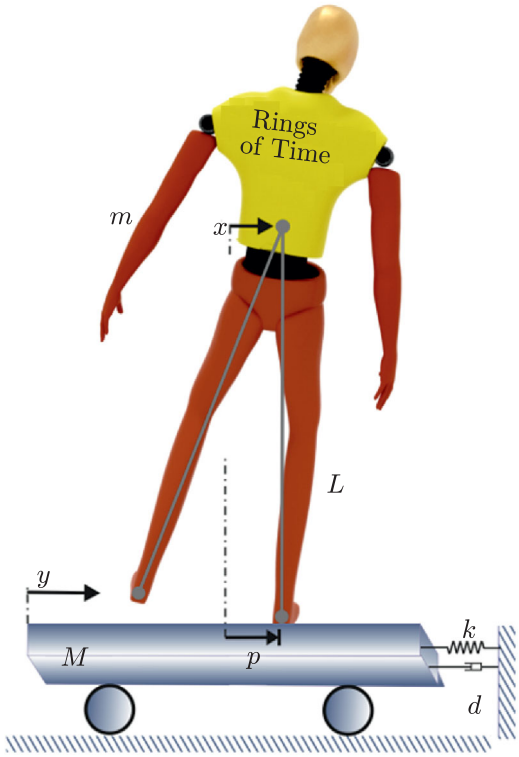

Fig. 1. Dynamical pedestrian–bridge model. Lateral oscillations of the pedestrian center of mass are modeled by an inverted pendulum of mass m and effective length L. The quantities x and p determine the lateral position of the pedestrian center of mass and the position of the center of pressure of the foot relative to the bridge, respectively. Bridge oscillations are modeled by a platform with mass M and a spring with constant k and damping coefficient d. The y coordinate corresponds to the bridge lateral displacement. We imagine this pedestrian as an M. I. Rabinovich poetry fan hurrying to the presentation of the "Rings on Time" book and walking along the UCSD-Scripps Crossing Pedestrian Bridge.

produce negative damping on average to make the bridge unstable over a wide range of bridge natural frequencies [18]. Paradoxically, pedestrians can stabilize bridge motion instead of shaking the bridge as one would expect.

In this paper, we first review recent results on the autonomous model of lateral motion of a single pedestrian, proposed in [32] and used to analyze large crowd dynamics in [26]. We then demonstrate the complexity of bidirectional interaction between a pedestrian and a light bridge by showing that there may be combinations of pedestrian and bridge frequencies that can lead to both negative and positive damping of bridge oscillations.

We devote this paper to the 80th birthday of M. I. Rabinovich, an outstanding scientist and a good friend of one of the authors (V. N. B). Like a pedestrian who can shake a bridge, M. I. Rabinovich's pioneering work has many times given momentum to a new development of nonlinear dynamics. The discovery of stable synchronization between chaotic systems [33] is only one of many examples that showcases M. I. Rabinovich's immense impact on modern physics and neuroscience.

The layout of this paper is as follows. In Sec. 2, we introduce an inverted pendulum model of pedestrian self-oscillatory motion. We first study the dynamics of the pedestrian on stationary ground, assuming no bridge motion. We derive equations for a stable limit cycle that controls the pedestrian's lateral gait and show how its amplitude and period depend on the parameters. In Sec. 3, we study pedestrian bridge interactions that can amplify or damp bridge oscillations depending on the frequency ratios. In Sec. 4, we provide concluding remarks and discuss the potential contribution of the single-pedestrian dynamics into overall, possibly incoherent crowd dynamics and bridge vibrations.

2. PEDESTRIAN–BRIDGE INTERACTION MODEL: INVERTED PENDULUM — LINEAR OSCILLATOR

We follow the standard approach [30–32] for modeling lateral oscillations of the bridge and transverse oscillations of the pedestrian center of mass by a mass–spring–damper system (Fig. 1).

The bridge is modeled by a platform of mass M with one side attached to a rigid support via an elastic

spring with constant k and a damper with damping coefficient d. Thus, the bridge motion is described by a damped linear oscillator, driven by the side-to-side motion of the pedestrian. The pedestrian is modeled by a self-oscillatory inverted pendulum, capable of adjusting the frequency and amplitude of steps in response to the lateral motion of the bridge. The pedestrian–bridge model is written as

$$\ddot{x} + f(x, \dot{x}) = -\ddot{y}, \qquad \ddot{y} + 2h\dot{y} + \Omega_0^2 y = -r\ddot{x}, \tag{1}$$

where x and y are lateral displacements of the center of mass of the pedestrian and the bridge, respectively, and the dots denote time differentiation. The self-oscillatory process and the response of the pedestrian motion to the bridge oscillations are modeled by the function $f(x, \dot{x})$. The term $-\ddot{y}$ accounts for an inertia force on the pedestrian movement caused by the bridge motion. The pedestrian applies force $-r\ddot{x}$ to the bridge. The pedestrian is assumed to have mass m and effective leg length L. Parameter $h = d/[2(M+m)]$ is the normalized damping coefficient, $\Omega_0 = \sqrt{k/(M+m)}$ is the natural frequency of the bridge loaded with one pedestrian, and parameter $r = m/(M+m)$ quantifies the strength of pedestrian–bridge interaction.

Many studies in bio-mechanics have indicated that an inverted pendulum model [18, 31, 32, 34] can successfully be applied to the analysis of the whole body balance in the lateral direction of human walking [35–37]. This class of inverted pendulum models can be described by various forms of the function $f(x, \dot{x})$, which determines the dynamics of the pedestrian center-of-mass lateral oscillations [18, 30–32].

In this paper, we use the autonomous walking model developed in [26, 32], which describes human walking as a process in which the stance leg acts as a rigid strut, making the pedestrian's center of mass act like an inverted pendulum during each step. The pedestrian switches legs when the position of his or her center of mass crosses a reference point $x = 0$. This model ignores the brief phase of weight transfer from one foot to the other. The adaptation function has the form

$$f(x, \dot{x}) = \lambda \left\{ \dot{x}^2 + \omega_0^2 \left[a^2 - (x - p \operatorname{sgn} x)^2 \right] \right\} \dot{x} - \omega_0^2 (x - p \operatorname{sgn} x), \tag{2}$$

where $\operatorname{sgn} x = -1$ if $x < 0$ and $\operatorname{sgn} x = 1$ if $x \geq 0$. The presence of the sgn function in (2) accounts for reversing the direction of movement of the pedestrian center of mass x when the pedestrian shifts the body's weight from one foot to the other. The quantities λ, a, p, and ω_0 are parameters of the problem, where λ corresponds to damping, a controls the self-oscillation amplitude, p is the horizontal displacement of the center of pressure of the foot, and $\omega_0 = \sqrt{g/L}$, where g is the acceleration due to gravity and L is the distance from the center of mass to the center of pressure (leg length).

In radiophysics terms, the pedestrian–bridge interaction described by system (1) is analogous to the dynamics of a nonlinear generator (the pedestrian) with an additional linear RLC circuit (the bridge). Such oscillatory radiophysical systems are known to exhibit frequency entrainment and bistability whose studies date back to Van der Pol, Andronov [38], and Teodorchik [39] (see a Physics Encyclopedia entry by V. N. Belykh and M. I. Rabinovich [40]). As in its radiophysical counterpart, the pedestrian–bridge interactions can also lead to bistability and hysteretic transitions between two stable oscillatory states. These states represent two co-existing pedestrian gaits that correspond to walking out of phase with the bridge. One of these gaits can induce significantly stronger bridge oscillations. A single misstep can change the initial conditions and force the pedestrian to switch to the other gait [32].

3. PEDESTRIAN GAIT ON THE MOTIONLESS BRIDGE

Before assessing the role of the pedestrian step frequency in influencing bridge oscillations, we study how intrinsic parameters of adaptation function (2) control the size and period of pedestrian lateral oscillations in the absence of bridge movement. Setting $\ddot{y} = 0$ in the first equation of (1), we decouple the system and obtain the equation of unperturbed pedestrian motion

$$\ddot{x} + \lambda \left\{ \dot{x}^2 + \nu^2 \left[a^2 - (x - p \operatorname{sgn} x)^2 \right] \right\} \dot{x} - \omega_0^2 (x - p \operatorname{sgn} x) = 0. \tag{3}$$

Note that this is a nonlinear piecewise-smooth model with a van der Pol-type self-sustained oscillatory mechanism. This piecewise-smooth model switches between two nonlinear equations for $x < 0$ (the left stance leg) and $x > 0$ (the right stance leg). A remarkable feature of this model is that, in contrast to its counterparts like the van der Pol-type equation, it allows finding an explicit solution in the form of a stable limit cycle, thereby yielding analytical expressions for the limit cycle amplitude and period as functions of the parameters [32].

3.1. Amplitude and period of pedestrian lateral oscillations

Let us formulate and prove the following two assertions.

1. Piecewise-smooth system (3) has a unique stable limit cycle with $x(t)$ and $\dot{x}(t)$ defined by

$$x = [p - a\cosh(\omega_0 t)]\,\mathrm{sgn}\,x, \quad \dot{x} = -a\omega_0 \sinh(\omega_0 t)\,\mathrm{sgn}\,x. \tag{4}$$

2. The period of the limit cycle is

$$T \equiv \frac{1}{\omega_1} = \frac{4}{\omega_0}\ln\left(p/a + \sqrt{(p/a)^2 - 1}\right). \tag{5}$$

The x- and $\dot{x}$-amplitudes of the limit cycle are $p - a$ and $a\omega_0 \sinh(\omega_0\tau)$, respectively.

The proof of these assertions can be constructed as follows.

For convenience, system (3) can be re-written in the form

$$\begin{aligned} &\dot{x} = u, \\ &\dot{u} = -\lambda\left\{\dot{x}^2 + \omega_0^2\left[a^2 - (x - p\,\mathrm{sgn}\,x)^2\right]\right\}u + \omega_0^2(x - p\,\mathrm{sgn}\,x). \end{aligned} \tag{6}$$

We choose

$$V = u^2 - \omega_0^2(x - p\,\hat{\mathrm{sgn}}\,x)^2 + \omega_0^2 a^2 \tag{7}$$

as a candidate Lyapunov function V to prove the uniqueness and stability of the limit cycle in system (6) in the region of interest $|x| < p$. Note that the level $V = 0$ that yields a closed curve is a Hamiltonian level in the conservative system (6) with $\lambda = 0$ (see [32] for details). We also notice that within the region of interest $|x| < p$, V is positive (negative) for x and u, lying outside (inside) the level curve $V = 0$. The limitation $|x| < p$ ensures the pedestrian balance control, since for $|x| > p$ the pedestrian inevitably falls in the lateral direction. The points $(x = p, u = 0)$ and $(x = -p, u = 0)$ are saddle fixed points of system (6) that limit the domain of attraction (see Fig. 2 in [32]).

The derivative of V along the trajectories of system (6)

$$\dot{V} = -2\lambda u^2 V \tag{8}$$

is negative (positive) definite when V is positive (negative). As a result, the trajectories of system (6) converge to the level $V = 0$ which represents a unique, stable piecewise-smooth limit cycle (see Fig. 2).

The solution of the differential equation that corresponds to $V = 0$,

$$(\dot{x})^2 = \omega_0^2(x - p\,\mathrm{sgn}\,x)^2 - \omega_0^2 a^2, \tag{9}$$

is given by $x = \mathrm{sgn}\,(p - a\cosh\omega_0 t)$. This solution yields the limit cycle (4).

Using (4), we calculate the period T of the limit cycle. The motion along the limit cycle from the point $x = p - a$ and $\dot{x} = 0$ to the point

$$x = 0, \quad \dot{x} = a\omega_0 \sinh(\omega_0\tau) \tag{10}$$

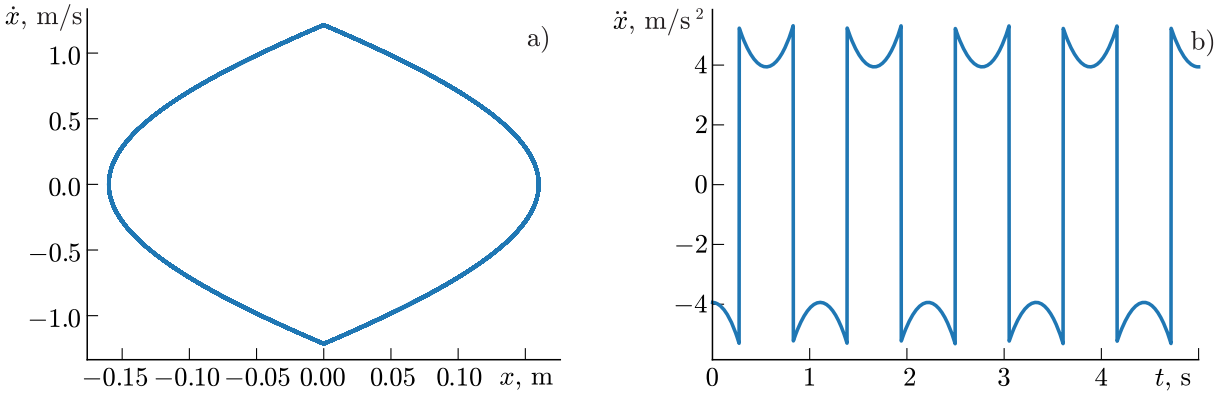

Fig. 2. (a) The limit cycle in the pedestrian model (3) in the absence of bridge oscillations. The non-smooth shape of the limit cycle is due to the switching from one leg to the other at $x = 0$. (b) The acceleration time series for pedestrian's lateral oscillations. Parameters are the damping due to walking $\lambda = 23.25$ cm^{-2}, pedestrian mass $m = 76.9$ kg, effective leg length $L = 1.17$ m, $p = 0.063$ m, $a = 0.047$ m, and $\omega_0 = \sqrt{g/L} = 2.89$ Hz.

comprises one-quarter of a period

$$\tau = \frac{1}{\omega_0} \ln\left(p/a + \sqrt{(p/a)^2 - 1}\right). \tag{11}$$

Formula (11) yields $T = 4\tau$ and the sought expressions for the x- and u- amplitudes of the limit cycle.

It follows from (3) that the period T of the limit cycle is controlled by parameters ω_0, p, and a, but this period is most sensitive to the ratio p/a. In particular, the period becomes very small for $a \to p$, so that the gait size in the direction transverse to the motion direction becomes very small and the pedestrian rapidly switches weight between legs. On the contrary, when $a \to 0$, the period becomes infinite, so the pedestrian never switches to the other leg. Thus, one can obtain the full range of pedestrian lateral oscillation frequencies, from zero to infinite, by simply varying the parameter a. Figure 2 demonstrates the limit cycle of system (3) together with its acceleration time series for realistic parameters of unperturbed human walking.

4. PEDESTRIAN–BRIDGE DYNAMICS

We now analyze how the ratio between the bridge natural frequencies and the frequencies of pedestrian's lateral oscillations influences the instability occurence.

The question of whether a pedestrian can excite bridge oscillations or damps them was recently addressed in [18] via assessing the mean negative damping. However, these calculations were performed for a pedestrian–bridge system, wherein the bridge motion was sinusoidal and independent from the pedestrian dynamics.

This setup corresponds to the low mass ratio (light pedestrian/heavy bridge), such that the force from a single pedestrian has a negligible effect on the bridge. However, for higher mass ratios the pedestrian–bridge interactions become significant and can produce various nonlinear effects in the bidirectionally coupled pedestrian–bridge system (1).

We perform the following numerical experiment. We choose pedestrian walk and bridge natural frequencies ω_1 and Ω_0 as control parameters and vary them to create a uniform multipoint grid of natural frequencies ω_1 and Ω_0, where Ω_0 ranges from 0.1 to 3 Hz and ω_1 ranges from 0.3 to 5.8 Hz.

For each point of the grid, representing a particular combination of parameters (ω_1, Ω_0), we numerically integrate system (1) with pedestrian initial conditions $x(0) = p - a$ (p=0.063 m, a=0.047 m) and $\dot{x}(0) = 0$ m/s and bridge initial conditions $y(0) = 0.03$ m and $\dot{x} = 0.03$ m/s for $t = 30$ s. We determine the average bridge amplitude $y_{\max}$ for the last 10 s and compute the mean frequencies of the pedestrian and

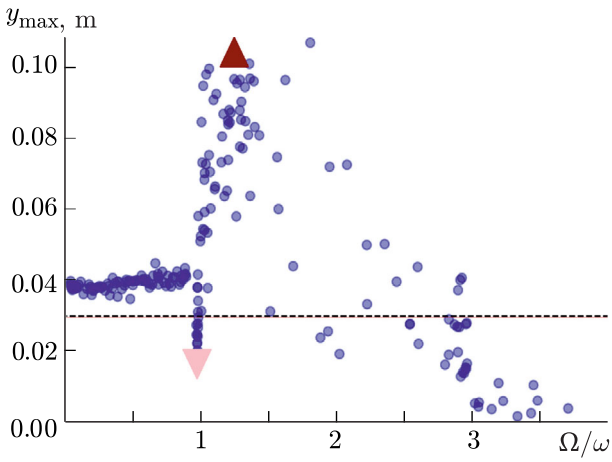

Fig. 3. Bridge amplitude $y_{\max}$ after the time $t = 30$ s as a function of 200 different combinations of bridge and pedestrian natural frequencies Ω_0 and ω_1, yielding frequency ratios Ω/ω. Here, Ω and ω are the numerically calculated bridge and pedestrian frequencies whose ratio corresponds to different combinations of Ω_0 and ω_1 (blue points). The dashed horizontal line represents the initial level of bridge oscillations with $y(0) = 0.03$ m and $\dot{y} = 0.001$ m/s. The thin red line corresponds to final $y_{\max} = 0.297$ after $t = 30$ in the absence of the pedestrian motion. The points above the red line indicate amplified pedestrian-induced bridge oscillations. The points below the red line yield combinations of Ω and ω for which the pedestrian damps the bridge oscillations. The points indicated by the red and pink triangles correspond to the maximum and minimum values of the amplitude resonance curve near the $1:1$ resonance. Other bridge parameters are $M = 3000$ kg and $h = 0.001$ N s/m. Pedestrian parameters are as in Fig. 2, except for varying ω_1. The integration step varies with an upper bound of 0.001.

bridge oscillations. These numerically calculated frequencies ω and Ω differ from the natural frequencies ω_1 and Ω_0 due to the bidirectional pedestrian–bridge interactions and the mutual adaptation of the pedestrian stride to the bridge motion, and vice versa. This leads to a non-uniform distribution of the blue points across the parameter range Ω/ω in Fig. 3. For a small bridge damping coefficient h typical of light rope bridges, the oscillations of the initially excited bridge decay very slowly in the absence of a pedestrian.

More specifically, the initial bridge amplitude $y(0) = 0.03$ m (depicted by a dashed black line in Fig. 3) only decays to $y(30) = 0.0297$ m (depicted by a red thin line, almost coinciding with the black line and barely seen in Fig. 3). Therefore, the points above (below) the red reference line indicate the amplification (suppression) of bridge oscillations by the pedestrian. Paradoxically, different combinations of Ω and ω yielding the same or close frequency ratios can either significantly enhance bridge oscillations (see, e. g., the red triangle) or damp them (the pink triangle). Remarkably, in both cases, the pedestrian and bridge are anti-phased; however, the amplitudes of the bridge and pedestrian stride differ significantly (see Fig. 4). The potential bistability of pedestrian lateral oscillations induced by bridge vibrations, which was analytically predicted in [32], can also be another factor supporting the co-existence of drastically different levels of bridge vibrations.

The non-uniform distribution of the points above and below the reference red line $y_{\max} = 0.0297$ m also indicates that a pedestrian can induce significant bridge instability outside the resonance-frequency range (see the cloud of points above the reference line in a wide range of Ω/ω from about 1 to 2).

5. CONCLUSIONS

Despite the significant interest of physicists and engineers, the understanding of how walking pedestrians and footbridges interact is far from being complete. In this paper, we have contributed to an improved understanding of the role of a single pedestrian in initiating or mitigating lateral bridge instabilities. We have used a dynamical model of an active inverted pendulum for lateral oscillations of the pedestrian center of mass to characterize how bridge oscillations can be enhanced or suppressed by resonance and non-resonance effects.

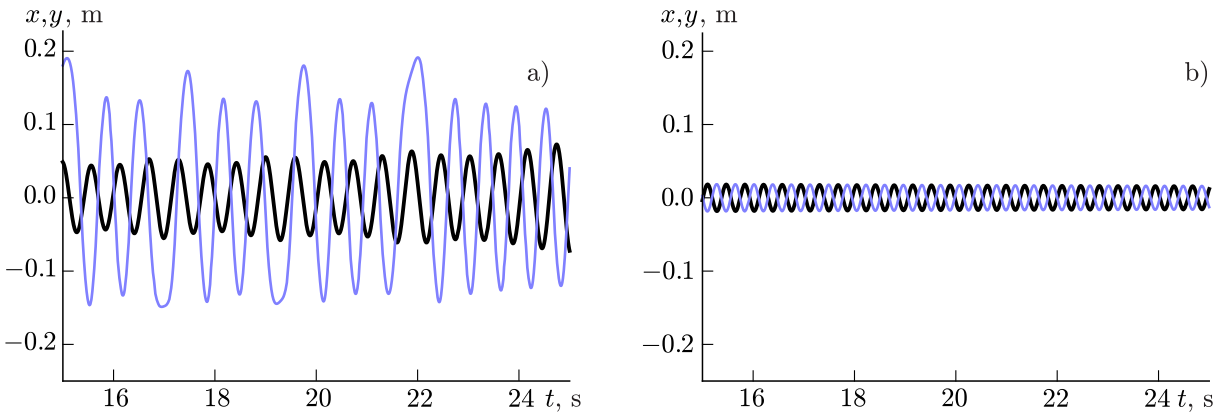

Fig. 4. Time series for the pedestrian center of mass $x(t)$ and bridge $y(t)$ oscillations (black and blue lines, respectively) for two combinations of Ω and ω corresponding to resonance values close to $\Omega/\omega = 1$. (a) $\Omega = 1.71$ and $\omega = 1.37$ (the red triangle in Fig. 3, the pedestrian amplifies bridge oscillations). (b) $\Omega = 2.68$ and $\omega = 2.72$ (the pink triangle in Fig. 3, the pedestrian contributes to the suppression of bridge oscillations).

We have shown a complex dependence of the bridge instability on the ratio between the pedestrian and bridge oscillation frequencies. Surprisingly, two different combinations of frequencies that yield the same or close ratios can lead to two distinct dynamical scenarios: one combination amplifies bridge oscillations, whereas the other suppresses them.

Remarkably, the frequency ratios that correspond to the bridge instability are not restricted to cases where the bridge oscillation frequency is close to pedestrian walking frequencies. Pedestrians with walking frequencies that fall into the stability or instability ranges may be present on a bridge, thereby pointing to the non-trivial problem of assessing the overall nonlinear impact of crowd dynamics on bridge instability. Our results and nonlinear models should enable bridge designers to better estimate the range of potentially dangerous frequency ratios and develop more accurate design criteria to avoid human-induced instability of a wide range of structures.

This work was supported by the Ministry of Science and Higher Education of the Russian Federation (project No. 0729-2020-0036, I. V. B. and V. N. B.), the Russian Science Foundation (project No. 19-12-00367, V. N. B.), and by the National Science Foundation (USA) (project No. DMS-1909924, I. V. B. and K. M. D.)

REFERENCES

1. Oeuvres Complétes de Christian Huygens. Publ. par la Sociètè hollandaise des sciences. Vol. 5, Correspondance 1664–1665, M. Nijhoff, La Haye (1893).
2. M. Bennett, M. F. Schatz, H. Rockwood, and K. Wiesenfeld, *Proc. Royal Soc. A: Math., Phys. and Engin. Sci.*, **458**, 563–579 (2002). https://doi.org/10.1098/rspa.2001.0888
3. A. Pikovsky, M. Rosenblum, and J. Kurths, *Synchronization: A Universal Concept in Nonlinear Sciences*, Cambridge University Press (2003).
4. J. Pena Ramirez, L. A. Olvera, H. Nijmeijer, and J. Alvarez, *Sci. Rep.*, **6**, 23580 (2016). https://doi.org/10.1038/srep23580
5. L. M. Pecora and T. L. Carroll, *Phys. Rev. Lett.*, **80**, 2109 (1998). https://doi.org/10.1103/PhysRevLett.80.2109
6. S. H. Strogatz, *Nature,* **410**, 268–276 (2001). https://doi.org/10.1038/35065725
7. S. Boccaletti, J. Kurths, G. Osipov, D. Valladares, and C. Zhou, *Phys. Rep.*, **366**, 1–101 (2002). https://doi.org/10.1016/S0370-1573(02)00137-0

8. V. N. Belykh, I. V. Belykh, and M. Hasler, *Phys. D: Nonlin. Phenom.*, **195**, 159–187 (2004). https://doi.org/10.1016/j.physd.2004.03.012

9. T. Nishikawa and A. E. Motter, *Proc. Nat. Acad. Sci. USA*, **107**, 10342–10347 (2010). https://doi.org/10.1073/pnas.0912444107

10. A. J. Whalen, S. N. Brennan, T. D. Sauer, and S. J. Schiff, *Phys. Rev. X*, **5**, 011005 (2015). https://doi.org/10.1103/PhysRevX.5.011005

11. H. Abarbanel, M. I. Rabinovich, A. Selverston, M. Bazhenov, R. Huerta, M. Sushchik, and L. Rubchinskii, *Phys. Usp.*, **39**, 337–362 (1996). https://doi.org/10.1070/PU1996v039n04ABEH000141

12. A. Szücs, R. Huerta, M. I. Rabinovich, and A. I. Selverston, *Neuron*, **61**, 439–453 (2009). https://doi.org/10.1016/j.neuron.2008.12.032

13. R. C. Elson, A. I. Selverston, H. D. Abarbanel, and M. I. Rabinovich, *J. Neurophys.*, **88**, 1166–1176 (2002). https://doi.org/10.1152/jn.2002.88.3.1166

14. R. Roy and K. S. Thornburg Jr., *Phys. Rev. Lett.*, **72**, 2009 (1994). https://doi.org/10.1103/PhysRevLett.72.2009

15. S. Shahin, F. Vallini, F. Monifi, et al., *Opt. Lett.*, **41**, 5238–5241 (2016). https://doi.org/10.1364/OL.41.005238

16. J. Ding, I. Belykh, A. Marandi, and M.-A. Miri, *Phys. Rev. Appl.*, **12**, 054039 (2019). https://doi.org/10.1103/PhysRevApplied.12.054039

17. A. E. Motter, S. A. Myers, M. Anghel, and T. Nishikawa, *Nat. Phys.*, **9**, 191–197 (2013). https://doi.org/10.1038/nphys2535

18. I. Belykh, M. Bocian, A. Champneys, et al., *Nat. Commun.*, **12**, 7223 (2021). https://doi.org/10.1038/s41467-021-27568-y

19. Y. Fujino, B. M. Pacheco, S.-I. Nakamura, and P. Warnitchai, *Earthquake Eng. Struct. Dyn.*, **22**, 741–758 (1993). https://doi.org/10.1002/eqe.4290220902

20. F. Danbon and G. Grillaud, in: *Proc. Footbridge-2nd Int. Conf. Dec., Venice, Italy*, 10075051 (2005).

21. P. Dallard, A. Fitzpatrick, A. Flint, S. Le Bourva, A. Low, R. Ridsdill Smith, and M. Willford, *Struct. Eng.*, **79**, 17–21 (2001).

22. S. Nakamura, *Struct. Eng.*, **81**, 22–26 (2003).

23. J. M. Brownjohn, P. Fok, M. Roche, and P. Omenzetter, *Struct. Eng.*, **82**, 21–27 (2004).

24. J. Macdonald, in: *Proc. Inst. Civil Engineers–Bridge Eng.*, **161**, No. 2, 69–77 (2008). https://doi.org/10.1680/bren.2008.161.2.69

25. E. Caetano, Á. Cunha, F. Magalhães, and C. Moutinho, *Eng. Struct.*, **32**, 1069–1081 (2010). https://doi.org/10.1016/j.engstruct.2009.12.034

26. I. Belykh, R. Jeter, and V. Belykh, *Sci. Adv.*, **3**, e1701512 (2017). https://doi.org/10.1126/sciadv.1701512

27. S. H. Strogatz, D. M. Abrams, A. McRobie, et al., *Nature,* **438**, No. 7064, 43–44 (2005). https://doi.org/10.1038/438043a

28. B. Eckhardt, E. Ott, S. H. Strogatz, et al., *Phys. Rev. E*, **75**, 021110 (2007). https://doi.org/10.1103/PhysRevE.75.021110

29. M. M. Abdulrehem and E. Ott, *Chaos*, **19**, 013129 (2009). https://doi.org/10.1063/1.3087434

30. J. H. Macdonald, *Proc. Roy. Soc. of London A: Math., Phys. Eng. Sci.*, **465**, 1055-1073 (2008).

31. M. Bocian, J. Macdonald, and J. Burn, *J. Sound Vibr.*, **331**, 3914–3929 (2012). https://doi.org/10.1016/j.jsv.2012.03.023

32. I. V. Belykh, R. Jeter, and V. N. Belykh, *Chaos,* **26**, 116314 (2016). https://doi.org/10.1063/1.4967725

33. V. S. Afraimovich, N. N. Verichev, and M. I. Rabinovich, *Radiophys. Quantum Electron.*, **29**, No. 9, 795–803 (1986). https://doi.org/10.1007/BF01034476

34. C. Barker, in: *Proc. Footbridge 1st Int. Conf., Paris, 20–22 November, 2002*, 10006505.

35. A. Hof, R. M. van Bockel, T. Schoppen, and K. Postema, *Gait and Posture*, **25**, No. 2, 250–258 (2007). https://doi.org/10.1016/j.gaitpost.2006.04.013

36. A. Hof, S. Vermerris, and W. Gjaltema, *J. Exper. Biol.*, **213**, 2655–2664 (2010). https://doi.org/10.1242/jeb.042572

37. C. D. MacKinnon and D. A. Winter, *J. Biomech.*, **26**, 633–644 (1993). https://doi.org/10.1016/0021-9290(93)90027-C

38. A. A. Andronov, A. A. Vitt, and S. E. Khaikin, *Theory of Oscillators*, Pergamon, London (1966).

39. K. F. Teodorchik, *Self-Oscillating Systems* [in Russian], Gostekhizdat, Moscow (1952).

40. V. N. Belykh and M. I. Rabinovich, in: *Fiz. Enzikl, Vol. 2,* Soviet Encyclopedia, Moscow (1990), pp. 38-39.